

Machine Learning Attack and Defense on Voltage Over-scaling-based Lightweight Authentication

Jiliang Zhang, *Member, IEEE*, Haihan Su

Abstract—It is a challenging task to deploy lightweight security protocols in resource-constrained IoT applications. A hardware-oriented lightweight authentication protocol based on device signature generated during voltage over-scaling (VOS) was recently proposed to address this issue. VOS-based authentication employs the computation unit such as adders to generate the process variation dependent error which is combined with secret keys to create a two-factor authentication protocol. In this paper, machine learning (ML)-based modeling attacks to break such authentication is presented. We also propose a dynamic obfuscation mechanism based on keys (DOMK) for the VOS-based authentication to resist ML attacks. Experimental results show that ANN, RNN and CMA-ES can clone the challenge-response behavior of VOS-based authentication with up to 99.65% predication accuracy, while the predication accuracy is less than 51.2% after deploying our proposed ML resilient technique.

Index Terms—Voltage over-scaling; Machine learning; Authentication; Obfuscation.

I. INTRODUCTION

The Internet of Things (IoT) is a novel networking paradigm which connects a variety of things or objects to the Internet through sensor technology, radio frequency identification (RFID), communication technology, computer networks and database technology [1]. According to the IHS forecast [2], the IoT market will grow from an installed base of 15.4 billion devices in 2015 to 30.7 billion devices in 2020 and 75.4 billion in 2025. With the increasing of IoT devices, security issues have attracted many attentions. For example, in 2016, America suffered the largest DDoS attack in history [3]. The cyber-attack that brought down much of America internet was caused by a new weapon called the Mirai botnet, which is a worm-like family of malware that infected IoT devices and corralled them into a DDoS botnet [4]. Therefore, efficient security defenses need to be deployed for IoT devices.

Secret key storage and device authentication are two key technologies for IoT security. Traditional key generation and authentication techniques are based on the classical cryptography, which requires expensive secret key storage and high-complexity cryptographic algorithms. In many IoT applications, resources like CPU, memory, and battery power are limited and cannot afford the classic cryptographic security

This work is supported by the National Natural Science Foundation of China (Grant No. 61602107), the National Natural Science Foundation of Hunan Province, China (Grant No. 61702107), the Fundamental Research Funds for the Central Universities, and special thanks to 2017 CCF-IFAA RESEARCH FUND for greatly supporting the writing of the paper.

J. Zhang and H. Su are with the College of Computer Science and Electronic Engineering, Hunan University, Changsha 410082, China (e-mail: zhangjiliang@hnu.edu.cn).

solutions. Therefore, lightweight solutions for IoT security are urgent.

Physical unclonable functions (PUFs) [5] and recently proposed voltage over-scaling (VOS) based authentication [6] are lightweight security primitives for IoT device authentication. Compared with the PUF, the VOS-based authentication has two advantages [6]: 1) lower power consumption; 2) no additional hardware required. Therefore, the VOS-based authentication is more suitable for resource-constrained IoT applications. VOS is a common power reduction technology in the approximate computing [9]. The calculation unit of digital circuits can generate correct results for all inputs under the normal operating voltage, but calculation errors may occur in VOS [7]. Meanwhile, the errors generated by the computing unit in VOS are related to the manufacturing process variation. Therefore, the errors can be used as hardware fingerprints for device authentication. Recently, Arafin, Gao and Qu [6] proposed to use such errors generated by the computing unit in VOS as the device signatures and designed a two-factor authentication protocol, named voltage over-scaling-based lightweight authentication (VOLtA).

However, this paper proves that the VOLtA is vulnerable to machine learning (ML) attacks, and in order to resist ML attacks, we propose a dynamic obfuscation mechanism based on keys (DOMK) for VOLtA. The main contributions of this paper are as follows.

- 1) We re-evaluate the security of VOLtA. For the first time, we demonstrate that ML attacks such as artificial neural network (ANN), recurrent neural network (RNN) and covariance matrix adaptation evolution strategy (CMA-ES) can break VOLtA successfully. Especially, the prediction accuracy of RNN is up to 99.65%.
- 2) We propose a DOMK-based ML resistant authentication protocol that reduces the prediction accuracy of ML modeling to less than 51.2%.
- 3) The VOS-based two-factor authentication scheme requires a very long key to encrypt the output, which incurs unacceptable key storage overhead. Our proposed DOMK-based ML resistant authentication protocol eliminates such weakness.

II. PRELIMINARIES

This section will introduce the principle of generating calculation errors in the VOS circuit.

A. Voltage Over-scaling

In digital signal processing systems, the power consumption P is given by:

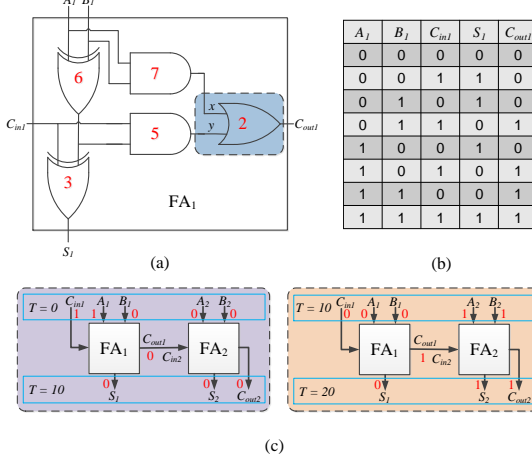


Fig. 1. An example of computing error. (a) The gate circuit of a full-adder. (b) The truth table of the full-adder. (c) The generation process of computing errors. A n -bit RCA is connected by n full-adders, and 2-bit RCA is depicted in (c).

$$P = C_L V_{dd}^2 f_s \quad (1)$$

where V_{dd} is the supply voltage; C_L is the effective switching capacitance; f_s is the clock frequency of circuit [7]. The circuit delay τ_d is given by:

$$\tau_d = \frac{C_L V_{dd}}{\beta(V_{dd} - V_t)^\alpha} \quad (2)$$

where α is the velocity saturation index, β is the gate transconductance and V_t is the device threshold voltage [6]. We can see from the Eqn. (1) and (2) that power consumption will decrease quadratically and the delay will increase dramatically with the decreasing of supply voltage [10]. With the correct timing constraints, the circuit produces correct outputs for all inputs. However, when the operating voltage is lowered, the timing violations may incur calculation errors. In the approximate computing, the computing unit performs high-bit calculations in the normal voltage and calculates low-bits in VOS, which not only makes the circuit generate approximate results but also significantly reduces the power consumption [9]. Furthermore, the errors produced by the process variation are random and can be reproduced by the original device but difficult to be cloned. Therefore, the errors can be used as the hardware fingerprints to authenticate the devices.

B. Computing Errors

As a common computing unit in digital circuits, Ripple Carry Adder (RCA) has the potential to preserve process variation related artifacts [6]. The principle of errors caused by the circuit delay is described in Fig. 1. The gate circuit and truth table of a full-adder (FA) are shown in Fig. 1(a) and Fig. 1(b), respectively. Fig. 1(c) gives the process of generating computing errors, where FA₁ is a simplified diagram of Fig. 1(a). For ease of exposition, we assume that the red numbers marked in Fig. 1(a) are the signal transmission delays of the logic gates, and there is no delay in FA₂. In Fig. 1(c), when the

clock period of the input signal is ‘10’, the first clock period is as follows.

- At time $T = 0$, the input pulse signal $\{C_{in1}, A_1, B_1, A_2, B_2\} = \{1, 1, 0, 0, 0\}$;
- At time $T = 10$, since the delay $D_y = 6 + 5 > 10$ at the y -input of OR gate, the signal ‘1’ is not yet transmitted to y -input, hence the signal at y -input is still ‘0’. The x -input of OR gate delay $D_x = 7 < 10$, the signal ‘0’ is transmitted to x -input successfully, and thus the C_{out1} -output of OR gate is ‘0’. The output $\{S_1, S_2, C_{out2}\} = \{0, 0, 0\} \neq \{0, 1, 0\}$, the first clock period is over.

The second clock period is as follows.

- At time $T = 10$, the input pulse signal $\{C_{in1}, A_1, B_1, A_2, B_2\} = \{0, 0, 0, 1, 1\}$;
- At time $T = 20$, since $D_y = 6 + 5 < 20$, the signal ‘1’ of the first clock period is transmitting in C_{out1} , and thus the output $\{S_1, S_2, C_{out2}\} = \{0, 1, 1\} \neq \{0, 0, 1\}$.

As discussed above, the errors produced by the adder in VOS are related to the current input and the previous inputs.

III. SECURITY ANALYSIS AND MODELING ATTACKS ON VOLTA

This section will analyze the security of VOLTA in detail, and then several ML attacks are proposed to model VOLTA.

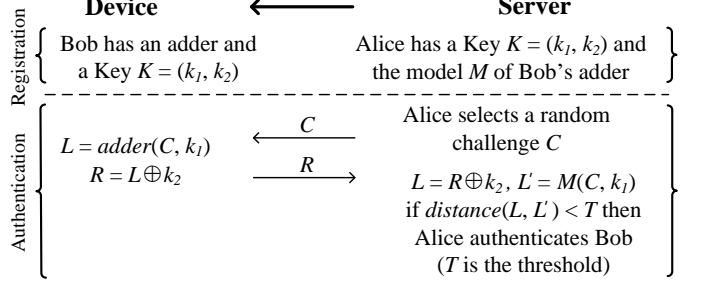


Fig. 2. The voltage over-scaling-based lightweight authentication protocol [6], where $adder()$ is the function of adder in VOS and $distance(L, L')$ can be measured by common distance measurement functions such as Hamming distance or Euclidean distance.

A. Security Analysis for VOLTA

The VOLTA is illustrated in Fig. 2, devices must have the adder and the correct key K , otherwise the authentication would be fail. However, the constant key has low obfuscation ability. Besides, the adder in VOS (VOS-adder) is vulnerable to ML attacks. Therefore, VOLTA suffers the security issues which will be discussed below.

1) Security Analysis of Constant Key

As shown in Fig. 1(a), the inputs of full-adder are $\{A_1, B_1, C_{in1}\}$, and the outputs are $\{S_1, C_{out1}\}$. Assume that the key k_1 is input to A_1 and the random challenge C is input to B_1 . For 1-bit calculation, the input A_1 is unchanged because k_1 is constant. We can see from Fig. 1(b), if $A_1 = 0$, then $S_1 = B_1 \oplus C_{in1}$ and $C_{out1} = B_1 \& C_{in1}$; if $A_1 = 1$, then $S_1 = !(B_1 \oplus C_{in1})$ and $C_{out1} = B_1 | C_{in1}$. The full-adder only implements the functions of two logic gates after using

the constant key k_1 , which does not increase the difficulty of modeling authentication protocol. We need to model a full-adder without the constant key k_1 . When the constant key k_1 is used, we only need to model the combination of two logic gates. Besides, the VOLtA uses the key k_2 to obfuscate the output. In what follows, we will further discuss the obfuscation effectiveness of the key k_2 .

Assume that $R = L \oplus k_2$, for 1-bit calculation, if $k_2 = 0$, then $R = L$; if $k_2 = 1$, then $R = \neg L$, which shows that when the output is obfuscated by the constant key, the i -th bit output is always unchanged or flipped. For instance, when the adder calculates 4 times, the outputs are $L_{1 \sim 4} = \{1011_1, 0011_2, \dots, 1010_8\}$, the key $k_2 = \{1_1, 0_2, \dots, 1_8\}$, and the responses $R_{1 \sim 4} = \{0100_1, 0011_2, \dots, 0101_8\}$ after using the XOR obfuscation. Obviously, when the i -th bit key $k_{2,i} = 1$, the i -th bit response is inverted such as the underlined parts of $R_{1 \sim 4}$; when the i -th bit key $k_{2,i} = 0$, the i -th bit response remains unchanged. We just need to establish a ML model for the i -th bit output to implement similar functions.

As analyzed above, the mechanism that employs constant keys to obfuscate the output is unable to resist ML attacks.

2) Complexity of Challenge-response Mapping

The VOLtA employs the CRPs to authenticate devices. The mapping of challenge-response (CR) depends on the calculation errors generated by a VOS-adder. As long as effective and enough CRPs are collected, ML algorithms can model the VOS-adder to simulate its CR behavior. In the VOLtA [6], assume that the length of the random challenge C is $8*n$ bits, the K is $16*n$ bits (k_1 and k_2 are both $8*n$ bits), which incurs unacceptable key storage overhead. For example, if a $52*40$ pixels image is used as the challenge for authentication, the required key K will be $16*52*40 = 33,280$ bits. In the case of ignoring the key storage overhead, we discuss the complexity of CR mapping.

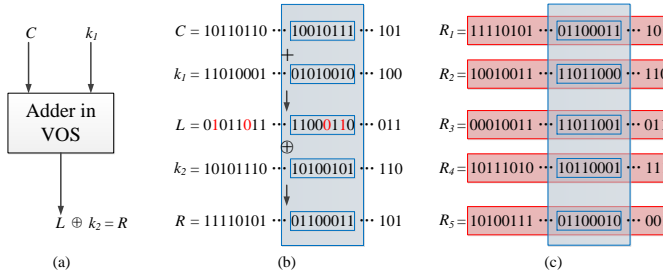


Fig. 3. A calculation example of VOLtA. In Fig. 3(a), the challenge C and the key k_1 are calculated by the VOS-adder to generate L , then L and the key k_2 are XORed to generate response R . Fig. 3(b) gives an example of the computing process, in which the red numbers indicate the computing errors. Fig. 3(c) gives a response example of 5 times authentication. We call the data in red box as horizontal data, and the data in blue box as vertical data.

A calculation example of VOLtA is illustrated in Fig. 3. The adder performs each addition and XOR operation with the corresponding k_1 and k_2 . Therefore, the horizontal data is obfuscated by different keys so that horizontal data can not be used to train the model with high accuracy. However, from the perspective of vertical data, the key used by the i -th byte of C is the same for each time, and the calculation of the data in the blue box (see Fig. 3(b) and Fig. 3(c)) uses the same

key. Therefore, we can use the data in blue box to model the operation of its corresponding byte, and the VOLtA can be modeled using valid CRPs with high prediction accuracy.

B. Modeling Attacks on VOLtA

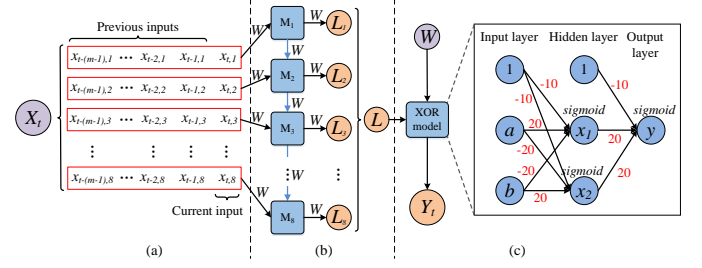


Fig. 4. The attack model of VOLtA.

As analyzed above, we first need to model the logic gates. The common logic gates include NOT gate, AND gate, OR gate and XOR gate, where the XOR gate is linearly inseparable and hence often is used to encrypt information in cryptography. However, the XOR can be implemented by other logic operations. For example,

$$a \oplus b = (a \& \neg b) | (\neg a \& b) \quad (3)$$

where ' \neg ' is NOT, ' $\&$ ' is AND, ' $|$ ' is OR and ' \oplus ' is XOR. Besides, NOT, AND and OR can be approximated as:

$$\neg a = 1 - a \quad (4)$$

$$a \& b \approx \text{sigmoid}(20 * a + 20 * b - 30) \quad (5)$$

$$a | b \approx \text{sigmoid}(20 * a + 20 * b - 10) \quad (6)$$

where $\text{sigmoid}(x) = 1/(1 + e^{-x})$, which is a common activation function in the neural network. Substituting Eqn. (4), (5) and (6) into Eqn. (3), the approximate expressions for XOR can be obtained. Based on this, we design the neural network structure shown in Fig. 4(c) to model the XOR gate, where $x_1 \approx a \& \neg b$, $x_2 \approx \neg a \& b$ and $y \approx x_1 | x_2$. To model the required functions, we expand the number of the hidden layer neurons to 10, and set the edges to random weight parameters to model any logic gate; when we model the obfuscation mechanism using the constant key, the weight parameters of edges is set to the red numbers in Fig. 4(c) and neuron b is set to a random parameter.

The attack model of VOLtA is shown in Fig. 4. Since the current output in VOLtA is related to the current input and the previous inputs, the input of model is adjusted to learn the effective mapping between input and output. As shown in Fig. 4(a), the current input is combined with the previous inputs to create the actual input $X_t = \{x_{t-(m-1)}, \dots, x_{t-2}, x_{t-1}, x_t\}$, where m denotes the number of input bytes, x_t denotes t timing input, and $x_{t-m,i}$ denotes the i -th bit of $t - m$ timing input. We use the vertical data to model the VOLtA. The neural network model of 8-bit Ripple Carry Adder (8-RCA) is shown in Fig. 4(b), the i -th bit of 8-RCA is input to M_i , and M_{i-1} is used as the input of M_i , which is a typical RNN structure.

The XOR obfuscation mechanism is shown in Fig. 4(c). All weight parameters W are random numbers that the ML model needs to adjust.

IV. ML ATTACKS RESISTANT AUTHENTICATION PROTOCOL

To resist ML modeling attack, this paper proposes a (DOMK)-based authentication protocol against ML attacks.

A. The DOMK

The errors generated by VOS-adder are related to input timing, and the current output is determined by the current input and the previous inputs. If the correlation among inputs is enhanced or the inputs are obfuscated, ML modeling attacks would be difficult.

This paper proposed a dynamic obfuscation mechanism based on keys (DOMK) to obfuscate challenges. The key idea of DOMK is to combine the previous inputs with secret keys to generate dynamic new keys, and exploit the new keys to obfuscate the current input. Assume that the challenge $C = \{c_1, c_2, \dots, c_n\}$, the keys are k_1 and k_2 , and the obfuscated challenge $C' = \{c'_1, c'_2, \dots, c'_n\}$ can be expressed as:

$$c'_i = k_1 \oplus g_i \quad (7)$$

$$g_i = f(c_1, k_{2,1}) \oplus f(c_2, k_{2,2}) \oplus \dots \oplus f(c_{i-1}, k_{2,(i-2)\%8+1}) \oplus c_i \quad (8)$$

$$f(x, y) = \begin{cases} x, y = 1 \\ 0, y = 0 \end{cases} \quad (9)$$

In Eqn. (8), a 8-bit key k_2 is used to obfuscate the intermediate calculation values $G = \{g_1, g_2, \dots, g_n\}$. For instance, if $k_2 = 10100101$, $g_6 = c_1 \oplus c_3 \oplus c_6$ and $g_7 = c_1 \oplus c_3 \oplus c_6 \oplus c_7$. In the authentication, the obfuscated challenge C' will be transmitted as the real challenge to the adder for calculation. Attackers can only collect the challenge C and the response corresponding to C' . In this case, the attackers cannot collect valid CRPs for ML modeling attacks.

B. Hardware Implementation

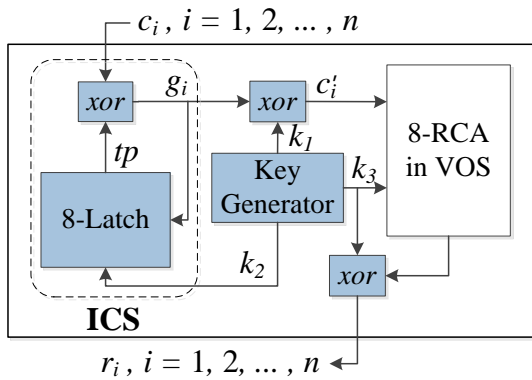


Fig. 5. The hardware implementation of DOMK.

As shown in Fig. 5, the DOMK structure proposed in this paper consists of 8 latches (8-latch), a key generator and

XOR gates. 8-latch is used to store g_i (see Eqn. (8)) in the calculation and the Key Generator is used to generate the secret key K . Besides, we design an input cache structure (ICS) to generate g_i . The ICS includes two operations:

- **Read-write operation:** 8-latch keeps latching state and outputs tp before calculating g_i , so that $g_i = c_i \oplus tp$. After calculating g_i , 8-latch is released from the latching state and then g_i is written into 8-latch, i.e., $tp = g_i$.
- **Hold operation:** 8-latch holds latching state and outputs tp throughout, $g_i = c_i \oplus tp$, and tp keeps unchanged until the next operation is performed.

The read-write and hold operations are controlled by a periodic signal based on the key k_2 . We assume $k_2 = 10100101$, and the control signals of ICS are 10100101 10100101 ... 10100101. If the control signal is '1', ICS performs the read-write operation; if the control signal is '0', ICS executes the hold operation. In this way, we get $G = \{g_1, g_2, \dots, g_n\}$ which is obfuscated by the key k_2 , and C' can be generated by the key k_1 .

C. Authentication Protocol

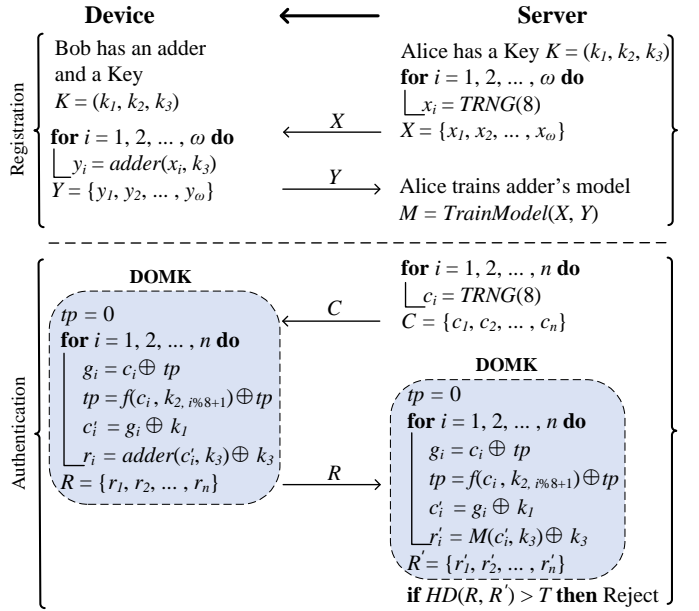


Fig. 6. The DOMK-based ML attacks resistant authentication protocol.

We propose a DOMK-based ML attacks resistant authentication protocol. The key K and the VOS-adder are used to authenticate devices. The key K consists of three different keys k_1 , k_2 and k_3 , where k_1 and k_2 are used to obfuscate the challenge in DOMK, and k_3 has two functions: 1) as one input of the adder; 2) encrypting the output of adder by XOR. The length of k_1 and k_3 are 8 bits, and k_2 can be any length (in this paper, k_2 is set to 8 bits). As shown in Fig. 6, the authentication protocol includes registration and authentication:

Registration

- i. Alice and Bob obtain the secret key $K = \{k_1, k_2, k_3\}$ through key sharing or other methods;

- ii. Alice randomly generates an input bits-stream $X = \{x_1, x_2, \dots, x_\omega\}$, where ω is the number of bytes of X , then sends X to Bob;
- iii. Bob adds x_i and k_3 using VOS-adder to get an output bit-stream $Y = \{y_1, y_2, \dots, y_\omega\}$, and sends Y to Alice;
- iv. Alice uses X and Y to train the adder model of Bob.

Authentication

- i. Alice generates a random challenge $C = \{c_1, c_2, \dots, c_n\}$, and sends it to Bob;
- ii. Bob employs DOMK to obfuscate challenge C to get the challenge $C' = \{c'_1, c'_2, \dots, c'_n\}$, and adds c'_i and k_3 using VOS-adder, then XORs the calculation result and k_3 to obtain the response $R = \{r_1, r_2, \dots, r_n\}$, and finally R is sent to Alice;
- iii. Alice obtains the obfuscated challenge C' through DOMK and C , then employs the model M and k_3 to generate the response R' ;
- iv. Alice calculates the Hamming distance $HD(R, R')$ between R and R' . If the $HD(R, R')$ is greater than the threshold condition, the authentication fails.

D. Security Analysis

1) *Key Security*: Our proposed DOMK combines the previous inputs with the secret keys to obfuscate the current input. If attackers know the key and the adder model, they can conduct replay attacks. Therefore, the server needs to ensure the security of keys and models. Moreover, the key generation module on the device can be the weak PUF [5] or the random number generator (RNG), which can prevent the attackers from stealing the keys from the device to restore the obfuscated challenge to perform ML modeling attacks.

2) *Brute Force Attacks*: Attackers enumerate the keys and build multiple models to attack. Assume that the keys k_1 and k_3 are 8 bits, k_2 is x bits, the number of models that attackers need to build to pass the authentication is $2^{(16+x)}$ which is increased exponentially with the increasing of x . Therefore, it is impossible for attackers to clone the DOMK-based authentication by brute-force attacks.

3) *Learning-based Attacks*: Attackers try to collect large amounts of data to conduct ML attacks. In the DOMK, the inputs in different timings are obfuscated by the changed keys, and the mapping of CRPs becomes highly complex. Therefore, it is difficult for attackers to model the DOMK-based authentication protocol without knowing the key and the adder model.

V. EXPERIMENTAL

A. Experimental Setup and Data Collection

In the experiments, we have reproduced the simulation experiment for a 8-RCA circuit in [6] and performed simulations in the HSpice platform using the FreePDK 45nm libraries [11]. The python 3.6.4 programming language and the tensorflow 1.6.0 neural network toolkit are used to conduct modeling attacks. All experiments are conducted on the Intel(R) Core(TM) i5-7400 CPU @ 3.00GHz, 8G RAM and GeForce GT 720 GPU.

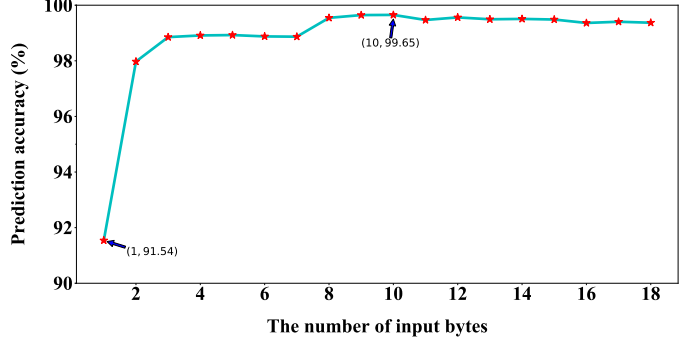


Fig. 7. Modeling accuracies of RNN on VOLtA with different numbers of input elements using 10,000 CRPs.

We modified the threshold voltages of the NMOS and PMOS models in the FreePDK 45nm libraries to simulate process variations based on the Gaussian distribution $\pm 7\%$. The circuit netlist for the 8-RCA is designed by using the modified NMOS and PMOS models at random, and then the circuit simulation was implemented in HSpice, where the simulation temperature is 25°C. We collected the challenge-response pairs (CRPs) generated by this 8-RCA to perform modeling attacks.

B. ML Attacks

In this section, ANN, RNN and CMA-ES are used to evaluate the effectiveness of modeling attacks, and RNN is used to attack the VOLtA and the no-key-VOLtA (VOLtA without two-factor). 20,000 CRPs for VOLtA and no-key-VOLtA are simulated by using HSpice. ML models are trained by using 10,000 CRPs and the rest of 10,000 CRPs are used as the testing set.

In the VOLtA, the current output of adder is related to the current input and the previous inputs. Therefore, the single input consists of multiple bytes, which is recorded as the input $X_t = \{x_{t-(m-1)}, \dots, x_{t-2}, x_{t-1}, x_t\}$. The single output is 1-byte representing the current output of adder. Fig. 7 shows the modeling accuracies of RNN on VOLtA with different input bytes using 10,000 CRPs. We use the Hamming distance to evaluate the modeling accuracy. We can see from Fig. 7 that when $m = 1$, only the current input is used as the training input, the prediction accuracy of RNN is only 91.54%. With the increasing of m , the modeling accuracy is also increased. The prediction accuracy reaches the highest 99.65% at $m = 10$. We take $m = 10$ to conduct the following experiments.

The results of ML attacks on VOLtA and no-key-VOLtA are shown in Fig. 8. When using the RNN to attack the no-key-VOLtA, we collect two inputs of the adder as the challenge. When collecting 500 CRPs, the modeling accuracy of RNN model is more than 90%; when collecting 10,000 CRPs, the prediction accuracy is up to 99.52%. Therefore, the no-key-VOLtA is vulnerable to ML attacks. Next, we use ANN, RNN and CMA-ES to attack VOLtA. Since the output and one input have been obfuscated by the key in VOLtA, we only collect one input of adder as the challenge and the obfuscated output as the response. When 5,000 CRPs are collected, the

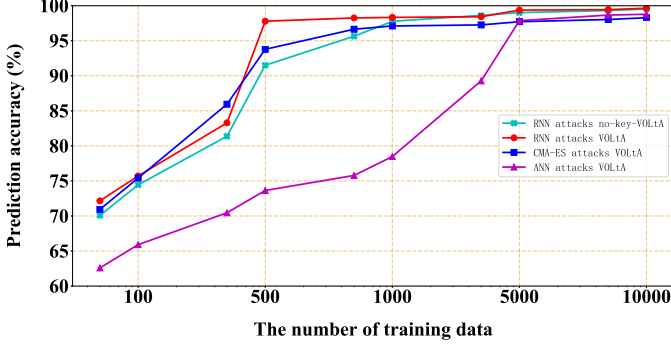


Fig. 8. Modeling accuracies for VOLtA and no-key-VOLtA using 10,000 CRPs.

modeling accuracies of ML attacks reach more than 95%; when collecting 10,000 CRPs, the prediction accuracy of RNN is up to 99.65%. Therefore, the modeling accuracy of RNN for VOLtA is just slightly higher than the no-key-VOLtA. In fact, the adder performs an approximate addition operation in VOS, where response $R = k_2 \oplus \text{adder}(C, X)$, if X is an input, attackers can guess k_2 according to large amounts of C , X and R ; if X is k_1 , this will reduce the complexity of the model but increase the model security. Besides, the attackers need to collect vertical data to attack VOLtA, which requires to collect more data and consumes more time.

C. VOLtA Reliability

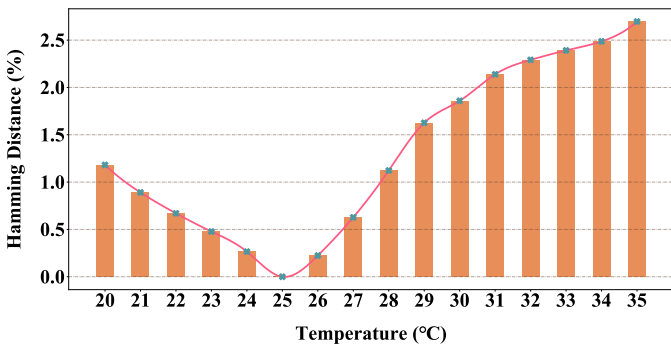


Fig. 9. Reliability impacted by temperature variation (nominal temperature is 25°C).

The intra Hamming distance (intra HD) of the responses is used to evaluate the reliability of VOLtA. We can see from Fig. 9 that the intra HD is around 0.47% when temperature decreases from 25°C to 23°C, and it is about 0.62% when temperature increases from 25°C to 27°C. The prediction accuracy of RNN is 99.65%, while the error generated by the RNN is only 0.35% which is less than the error caused by $\pm 2^\circ\text{C}$. Unfortunately, the setting of threshold in VOLtA must consider the influence of temperature and other factors on the reliability. When the threshold is determined, the ML models can reach the threshold condition as well. Therefore, the VOLtA is vulnerable to ML modeling attacks.

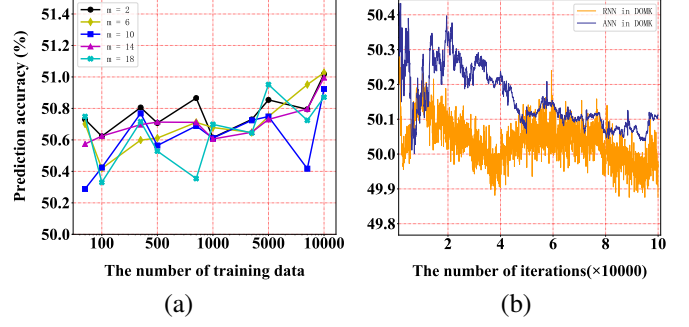


Fig. 10. The effectiveness of DMOK-based ML attacks resistant authentication.

D. Resistance to ML Attacks

The effectiveness of DMOK-based ML attacks resistant authentication is evaluated. As shown in Fig. 10(a), we set the input byte $m = 2, 6, 10, 14, 18$; the training set is from 50 to 10,000. RNN is used to verify the effectiveness of the proposed protocol, in which the prediction accuracy selects the maximum during training. From the experimental results we can see that even if the training set or m is increased, the modeling accuracy is between 50% and 51.2%. The relationship between the iterations and the modeling accuracy of ML methods is shown in Fig. 10(b). We can see that with the increasing of iterations, the prediction accuracies of ML methods are oscillating around 50.1%. Therefore, the proposed DMOK-based authentication exhibits good resilience to learning-based attacks.

VI. CONCLUSION

In this paper, we have re-evaluated the security of the VOS-based authentication protocol and implemented several high-accuracy ML modeling attacks on VOLtA. Experimental results show that the VOLtA is vulnerable to ML attacks, and the prediction accuracy of RNN is up to 99.65%. To resist the ML attacks on the VOLtA, this paper proposes a novel dynamic obfuscation mechanism based on keys (DOMK), which lowers the prediction accuracy of ML on the VOLtA to 51.2%.

REFERENCES

- [1] S. Li, L. D. Xu, and S. Zhao, "The internet of things: a survey," *Inf. Syst. Front.*, vol. 17, no. 2, pp. 243-259, Apr. 2015.
- [2] "Smart Summit Asia: Identifying Key Technology Drivers for Wider Adoption of Connected Solutions," [Online]. Available: <https://technology.ihs.com/587648>, 2017.
- [3] "DDoS attack that disrupted internet was largest of its kind in history, experts say," [Online]. Available: <https://www.theguardian.com/technology/2016/oct/26/ddos-attack-dyn-mirai-botnet>, 2016.
- [4] M. Antonakakis et al., "Understanding the Mirai Botnet This paper is included in the Proceedings of the Understanding the Mirai Botnet," *USENIX Secur.*, 2017.
- [5] J. L. Zhang, G. Qu, Y. Q. Lv, and Q. Zhou, "A survey on silicon PUFs and recent advances in ring oscillator PUFs," *J. Comput. Sci. Technol.*, vol. 29, no. 4, pp. 664-678, 2014.
- [6] M. T. Arafat, M. Gao, and G. Qu, "VOLtA: Voltage Over-scaling Based Lightweight Authentication for IoT Applications," *2017 22nd Asia and South Pacific Design Automation Conference (ASP-DAC)*. IEEE, pp. 336-341, 2017.

- [7] J. N. Chen and J. H. Hu, "Energy-Efficient Digital Signal Processing via Voltage-Overscaling-Based Residue Number System," *IEEE Trans. Very Large Scale Integr. Syst.*, vol. 21, no. 7, pp. 1322-1332, Jul. 2013.
- [8] J. Han and M. Orshansky, "Approximate Computing: An Emerging Paradigm For Energy-Efficient Design," *Test Symposium. IEEE*, vol. 370, pp. 1-6, 2013.
- [9] R. Venkatesan, A. Agarwal, K. Roy, and A. Raghunathan, "MACACO: Modeling and analysis of circuits for approximate computing," in *IEEE/ACM International Conference on Computer-Aided Design, Digest of Technical Papers, ICCAD*, pp. 667-673, 2011.
- [10] R. Liu and K. K. Parhi, "Power reduction in frequency-selective FIR filters under voltage overscaling," *IEEE J. Emerg. Sel. Top. Circuits Syst.*, vol. 1, no. 3, pp. 343-356, 2011.
- [11] J. E. Stine et al., "FreePDK: An Open-Source Variation-Aware Design Kit," *IEEE International Conference on Microelectronic Systems Education. IEEE*, pp. 0-1, 2007.